Title: Analysis of Laser Ablation Plumes by Laser-Induced Breakdown Spectroscopy and Quadrupole Mass Spectrometry: a Preliminary Study

Author names and affiliations: J.S. Cowpe[*a], J.S. Astin[a], R.D. Pilkington[a], A.E. Hill[a], M. Longson[b], T. Robinson[b]

[a] Institute for Materials Research, University of Salford, Salford, M5 4WT, UK.

j.s.cowpe@pgr.salford.ac.uk
r.d.pilkington@salford.ac.uk
j.s.astin@salford.ac.uk
a.e.hill@salford.ac.uk

[b] MKS Instruments UK Ltd, 2 St Georges Court, Hanover Business Park, Altrincham, Cheshire, WA14 5UA, UK.

Mark_Longson@mksinst.com
Tim_Robinson@mksinst.com

[*]**Corresponding author:** J. S. Cowpe. j.s.cowpe@pgr.salford.ac.uk
Institute for Materials Research, Room 105 Maxwell Building, University of Salford, Salford, M5 4WT, UK. Telephone: +44-161-295-5268

Abstract: Plasma plumes resulting from Nd:YAG laser ablation of copper and Fecralloy (Fe 72.8%, Cr 22%, Al 5%, Zr trace, Y trace) have been analysed simultaneously with Laser-Induced Breakdown Spectroscopy (LIBS) and Laser Ablation Mass Spectrometry (LAMS). A commercially available Residual Gas Analyser (RGA) was employed to perform mass spectrometric analysis of the neutral and ionic species created during the laser ablation process. Investigations of laser repetition rate have shown that increasing the frequency of the laser pulse rate is detrimental to the mass spectra produced; the average detectable partial pressure drops and the relative standard deviation of the signal increases. The RGA has been shown to be susceptible to corruption of measurement due to pump oil contamination when recording the partial pressure of neutral species created by the ablation event. Lack of

synchronisation between the transient laser pulse and the RGA mass scan results in variable partial pressure readings when analysing both neutral and ionic species. LAMS is able to detect small trace amounts of Zirconium and Yttrium in Fecralloy; LIBS is unable to resolve these trace amounts, but is shown to be unaffected by chamber pump oil contamination.

Keywords: LIBS, mass spectrometry, quadrupole, residual gas analyser, laser ablation

1. Introduction

1.1 Laser-Induced Breakdown Spectroscopy

Laser Induced Breakdown Spectroscopy (LIBS) is an atomic emission spectroscopy technique that employs a high powered, pulsed laser beam as the excitation source. LIBS historically has been a qualitative technique but over the last few years it has developed into a pseudo-quantitative materials micro-analysis technique, capable of determining the elemental composition of solids, liquids and gases [1]. The output of the laser is focussed onto the sample surface (or the effective surface for a gas) and if the fluence exceeds a certain threshold value (typically $\approx 10^8$ Wcm^{-2}; this value is material-specific [1]), then the analyte is ablated forming a plume propagating from the surface. This ablated material is composed of neutral particles, free electrons and highly ionised atoms, and expands as high temperature ($\approx 10^4$ K) plasma [2]. Spectroscopic analysis of the optical emission from the decaying species in the plume enables identification of the material under test.

Relatively poor sensitivity and complex matrix effects have hindered the quantitative application of LIBS [3]. The optical thickness of plasmas generated by laser ablation results in self-absorption of certain resonant emission lines, leading to non-linearity in the spectra produced [4]. Self absorbed spectral lines will have measured intensities lower than those predicted for a given elemental concentration; the observed elemental concentrations may differ from the actual composition of the analyte. For environmental monitoring, forensic applications and process control etc. this inaccuracy is unacceptable. Numerous calibration methods have been developed to counteract and correct for this effect [5], and several iterative calibration-free studies have and are being conducted [6]. Construction of calibration curves from standard samples [7, 8] requires a large number of reference samples for accurate calibration, which in the case of complex multi-elemental substances can be impractical and expensive. It can prove to be extremely difficult to analyse unknown samples if a suitable calibration has not been previously undertaken. Bulajic et al. [6] and Yaroschyk et al. [9] have shown that calibration-free methods require complex algorithms to generate predicted spectra. In order to examine a large wavelength range using a single spectrum, the resolution is necessarily reduced due to the coarser grating required. Identification of emission lines in complicated spectra can be problematic, resulting in inaccurate spectral interpretation that can lead to errors in compositional analysis.

This preliminary study was conducted to ascertain the viability of combining a relatively inexpensive quadrupole mass spectrometer with a LIBS system to resolve ambiguities that may exist within the LIBS spectrum.

1.2 Laser Ablation/Ionisation Mass spectrometry

Mass spectrometry (MS) has previously been coupled with laser ablation as a sampling method in Laser Ablation-Inductively Coupled Plasma-Mass Spectrometry (LA-ICP-MS) [10-13] and Matrix Assisted Laser Desorption-Ionisation (MALDI) [14,15] and also as an ionisation and sampling source for Laser Ablation Mass Spectrometry (LAMS) / Laser Ionisation Mass Spectrometry (LIMS) [16]. LIMS and LAMS are usually performed using expensive Time of Flight (ToF) MS analysis to overcome difficulties in synchronisation of a mass scan to the transient nature of a laser ablation event. Recent developments associated with the quadrupole mass spectrometer offer the potential for this small, relatively inexpensive instrument to be used as a flexible analytical tool.

Neutral species generated from laser ablation of polymers have been investigated [17] using quadrupole mass spectrometry. Ion energetics of ZnTe laser ablation plumes were measured using both ToF and quadrupole MS; the two techniques yielding comparable results [18]. Previous research combining results from simultaneous LIBS and MS have been restricted to the use of ToF analysis [19]. Several groups have applied a quadrupole mass filter to LIMS with varying degrees of success. Kuzuya et al. [20] employed a quadrupole mass filter to monitor the ion signals produced from laser ablation of metals, metal alloys and ceramics, obtaining reproducible spectra with less than 1% standard deviation in ion signal.

In this study we use a commercially available 300 amu MicroVision Plus Residual Gas Analyser (RGA) supplied by MKS Spectra.

2. Experimental setup

The apparatus shown schematically in Fig 1, allows the simultaneous LIBS and LA-MS investigation of solid or gas analytes. The system features a Surelite Continuum Nd:YAG laser, frequency doubled to produce an output at 532 nm, with 4-6 ns pulse length and a peak power of 200 mJ. The laser acts as both an excitation source for LIBS and a sampling method to volatise the analyte into the gaseous phase for introduction into the RGA. For most of the LIBS/LAMS experiments described here the laser was operated at a repetition rate of 1Hz unless otherwise specified. Laser radiation was focussed onto a sample using a 300 mm convex lens mounted on a micrometer stage, allowing positional adjustment along the axis of the laser beam (30mm either side of the focal position). Samples were positioned at the focal point of the focussing lens.

LAMS must be conducted under vacuum conditions, $<10^{-4}$ mbar, to prevent damage to the RGA; therefore the sample was mounted on an x-y stage within a vacuum chamber. The laser was focussed onto the material under test inside the chamber through a quartz window mounted in a Con-Flat carrier. A Leybold TurboVac 50 turbo-molecular pump backed by a Leybold TriVac rotary pump was used to evacuated the chamber to pressures $<10^{-6}$ mbar. A molecular sieve foreline trap was employed to help reduce pump oil vapour contamination back-streaming into the chamber.

Optical emission from the plasma plume was collected through a two metre fibre-optic cable manufactured by Roper Scientific that has a wavelength range of 190 to 1100 nm and a maximum collection angle of 25°. The fibre-optic cable was inserted into the vacuum chamber using a specially designed, elastomer sealed feed-through and is coupled to an Acton Research Spectra Pro 500i 0.5m imaging triple grating (150, 600, 2400 gmm^{-1}) spectrometer. The output of the spectrometer was coupled to a Princeton Instruments PI-MAX ICCD camera that utilises a proximity focussed MCP intensifier connected via a fibre-optic to a CCD array. The 1024x256 pixel CCD array is thermoelectrically cooled. A 1 ns increment in the gate delay and width was possible with a resolution of 40 ps. The laser power supply, camera and PC are connected to a Princeton Instruments ST-133A programmable timing generator which enables temporal resolution of the plasma plume. Roper Scientific's WinSpec/32 software allows both the capture of the optical emission and identification of the peaks recorded.

All experiments were conducted with a spectrometer gain of 100, 10 spectrum accumulations, camera gate delay of 600 ns, camera gate width of 800 ns and spectrometer input slit width of 70 μm. The x-y stage was used to move to a fresh spot on the sample for each analysis.
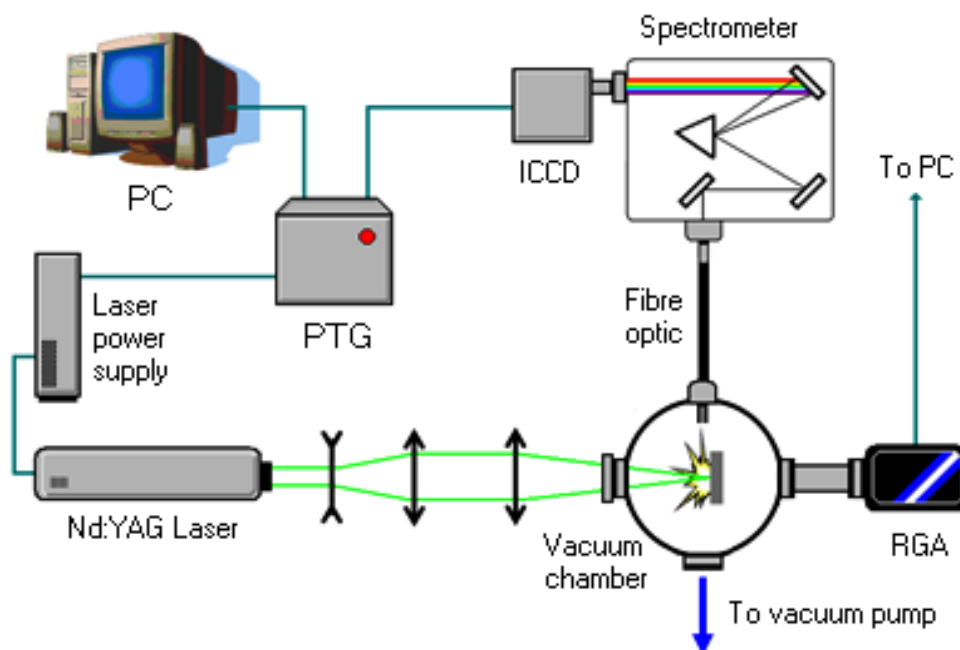

Figure 1: Schematic diagram of the combined LIBS/LAMS apparatus.

Analysis of the gaseous species within the vacuum chamber was conducted using an MKS MicroVision Plus 300 amu Residual Gas Analyser (RGA) with integer mass resolution. The RGA was mounted vertically at the base of the chamber and so was not in direct line-of-sight of the laser ablation plume; therefore the RGA does not sample the plume directly, but rather analyses the residual gases present in the chamber and monitors their respective partial pressures. The RGA is controlled using MKS Instruments' Process Eye Professional v5.22.0 software and the data obtained manipulated using MKS Instruments' Recall v5.22.0 software.

The RGA possesses an integral hot filament ion source which ordinarily ionises neutral species by electron bombardment for subsequent analysis. These ions are separated according to their mass to charge ratio (m/z) by the quadrupole mass analyser. Externally ionised particles are repelled by the RGA's ion optics; removal of the ion optics and filament ion source enables analysis of ions created during the ablation event. For any given ablation event, the RGA may be configured to analyse either the neutral

species or the ions within the plume. The RGA was programmed to scan repeatedly through a range of m/z ratios; an increase in the partial pressures of the gaseous species inside the chamber was observed as the laser was fired. It is inferred that the increased gas load was due to the ablation of the target material, and thus may be analysed to determine the composition of the sample.

When recording over large mass ranges the scan time of the RGA is long (10.52 seconds for a full 300 amu scan) compared with the transient laser ablation event. To increase the scan frequency and accuracy only masses known to be of interest were monitored. Initial background spectra were obtained before laser ablation of the sample was carried out. 100 laser pulses were fired and changes in the partial pressures of the masses of interest recorded over time. It was assumed that the sample materials used were homogeneous and that no compositional change with depth due to laser drilling occurred. All mass spectra were captured using a gain of 20 k on the Faraday cup detector, minimum detectable partial pressure 2.7×10^{-11} mbar.

Initial LIBS/LAMS investigations were conducted in order to determine whether the RGA was able to accurately discern the isotopic ratio of copper and validate the use of the system. The optimum repetition rate for the laser was found by performing LAMS of copper at various laser pulse frequencies. Simultaneous LIBS/LAMS analysis of Fecralloy (Fe 72.8%, Cr 22%, Al 5%, Zr trace, Y trace) was conducted to determine whether either technique can be employed to detect trace amounts of minor elements in a major element matrix.

3. Results and Discussion

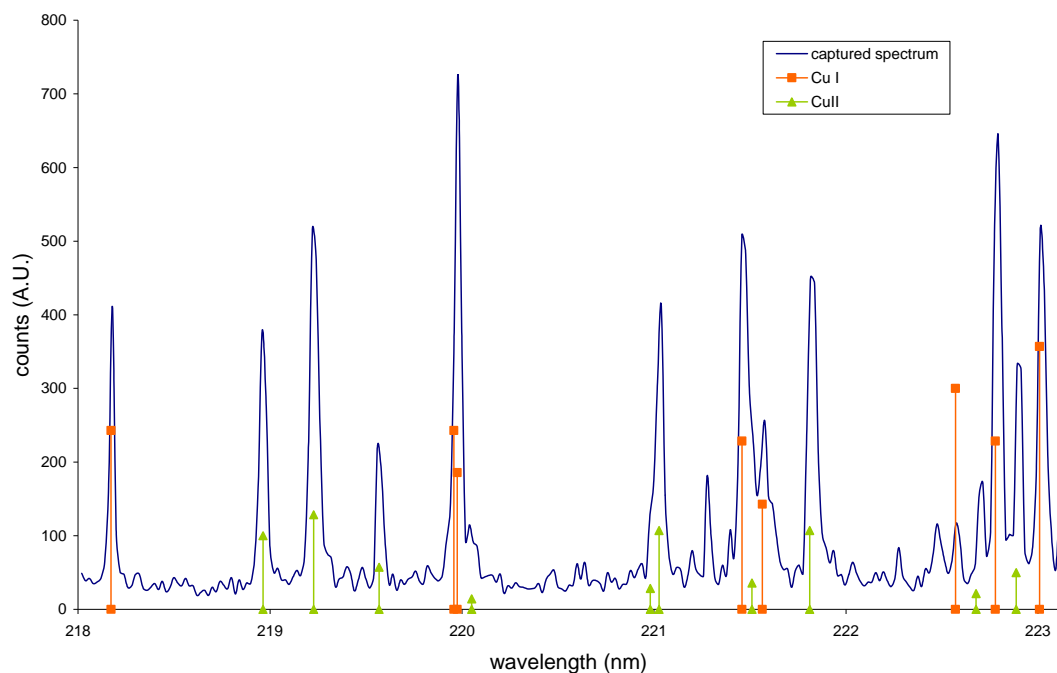### 3.1.1 Initial copper observations- LIBS

Figure 2. LIBS spectrum of Cu I and Cu II.

Figure 2 shows the LIBS spectrum captured during laser ablation of copper. Cu I and Cu II peaks are identified, indicating the presence of neutral and singly ionised species within the plasma plume (at a gate delay of 600ns, gate width 800ns). The peaks in the spectrum correlate closely to the predicted emission lines of copper; some evidence of self-absorption is observed e.g the line at 222.57 nm. The spectrum overlay represents the predicted relative intensity of each emission line; the mismatch between the observed and predicted intensities is due to the ratio of neutral to ionic species present at this stage of plume evolution. The neutral and ionic species in the plasma plume were subject to subsequent MS analysis.

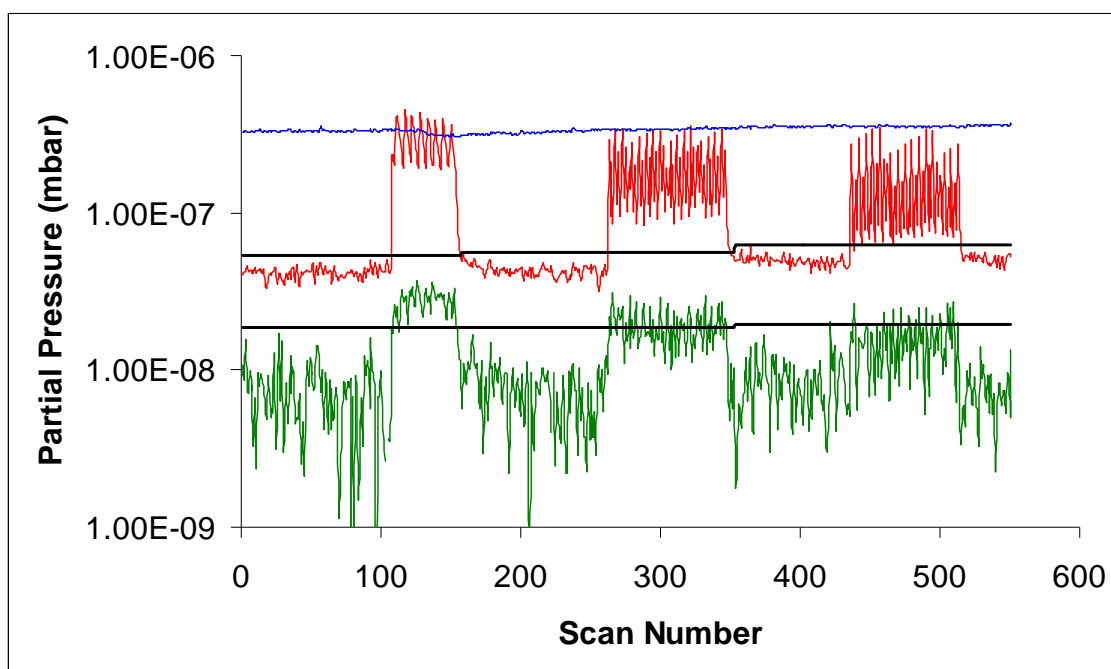### 3.1.2 Initial copper observations- MS

Figure 3. Partial pressures of 32 amu (top trace), 16 amu (middle trace) and 65 amu (bottom trace). Limits of detection for 16 amu and 63 amu are represented by the horizontal lines. Laser pulsed at repetition rates of 1, 5, 6.6 Hz (from left to right).

The plume resulting from laser ablation of copper was analysed using the RGA. Figure 3 shows the changes in partial pressure of the monitored masses against scan number from an experiment conducted as part of a preliminary investigation to determine the optimum repetition rate of the laser. These spectra were obtained using the RGA in normal mode to monitor neutral gas species. The bottom trace, mass 63 amu, is the major naturally abundant copper isotope; the minor isotope mass 65 amu was also monitored but is omitted from Figure 3 for clarity. The middle trace, mass 16 amu, may represent either atomic oxygen or a mechanical pump oil fragment CH_4. The top trace, mass 32 amu, molecular oxygen was monitored to confirm the origin of the 16 amu peak. It can be seen that the 32 amu trend remains at a constant average level while the 16 amu trend increases during the ablation process; this confirmed that pump oil contamination was present within the chamber. The three sets of peaks present on the 16 amu and 65amu traces are the signals recorded when the laser was fired at 1Hz, 5Hz and 6.6Hz (left to right). At frequencies greater than 6.6 Hz the pressure was seen to rise above the operating threshold of the RGA, due to the increased amount of material in the gaseous phase from laser ablation of the target material.

9

The horizontal lines across the 16amu and 63 amu traces represent the limits of detectable signal (LODS) for the given masses at their respective pressures. A detectable signal is defined as one being greater than 3 times the standard deviation of the background signal (laser not firing). Any signal lower than this cannot be resolved from the background noise. The background steadily rises after each run of laser shots due to the increased amount of gas phase ablated material in the chamber. The LODS was recalculated before each experiment to account for the variance in background level.

It can be seen that increasing the repetition rate of the laser is detrimental to the signal obtained. The mean detected partial pressure drops and the relative standard deviation of the signal increases, as shown in Figure 4.
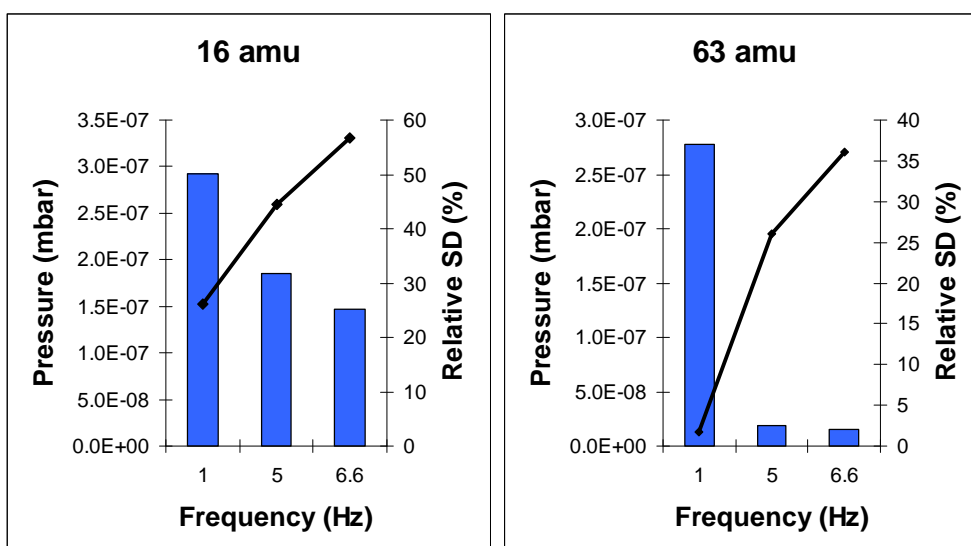

Figure 4. Mean detected partial pressure and relative standard deviation versus laser repetition rate, 16 amu (left) and 63 amu (right).

The 63 amu trace (Figure 3) is barely above the defined limit of detection with the laser pulsing at 6.6Hz. Operating the laser at higher pulse frequencies effectively lowers the sensitivity of the RGA. The rise in background signal on the 16 and 63 amu traces is due to the increased amount of each gaseous phase within the chamber as a result of the laser ablation process. The partial pressure of mass 16 features a 'saw tooth' profile which becomes more evident with increased laser pulse frequency. It is believed that this is due to a lack of synchronisation between the short laser pulse and the RGA mass scan (in this case 0.87 s at a minimum detectable partial pressure of 2.0×10^{-11} mbar).

A suitable timing and delay generator would solve this mismatch and should produce a steady partial pressure trace [20].
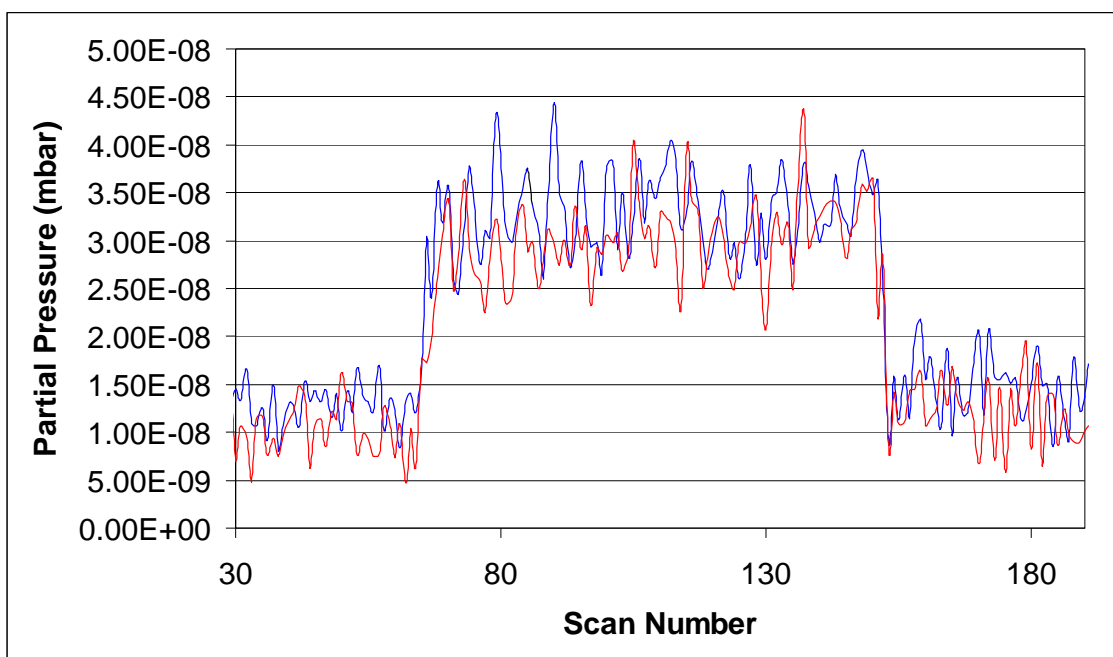

Figure 5. Partial pressure versus scan number, 63 amu and 65 amu, analysis of neutrals. 63 amu shown as the grey trace, 65 amu in black.

Figure 5 shows how the 63 and 65 amu partial pressures varying with scan number, with the laser operating at a repetition rate of 1 Hz, and an RGA scan time of 0.70 s. This spectrum was captured employing electron bombardment ionisation in order to analyse neutral species. In contrast, Figure 6 shows the analysis of ions present within the vacuum chamber, obtained with the RGA ionisation source and ion repeller plate removed and maximum potential applied to the ion accelerator plate. Figure 6 clearly shows the short-lived nature of these ions, and reveals that the analysis of the ablated ions presents a greater problem in terms of synchronising the laser pulse with the RGA mass scan than with analysis of neutrals.

At a pressure of $<10^{-6}$ mbar the gas molecules and ions present in the chamber are in the molecular flow regime, which implies that there are no interactions between the neutrals and ions, ions and ions etc. It should be noted that ion optics were not used to focus the ablated ions into the RGA, and therefore any ions entering the RGA do so in a random fashion. As the RGA was not positioned in direct line-of-sight of the ablated sample,

the number of ions entering the RGA is small compared to the number of ions colliding with the chamber walls and subsequently neutralised.
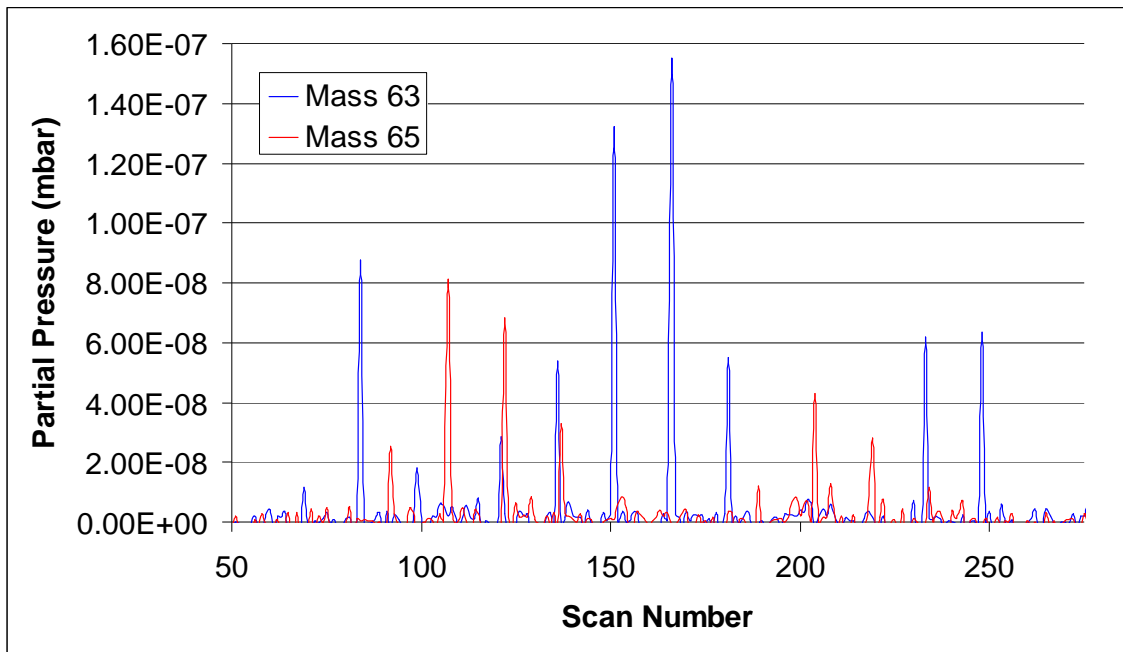

Figure6. Partial pressure versus scan number, 63 amu and 65 amu, analysis of ions. 63 amu shown as the grey trace, 65 amu in black.
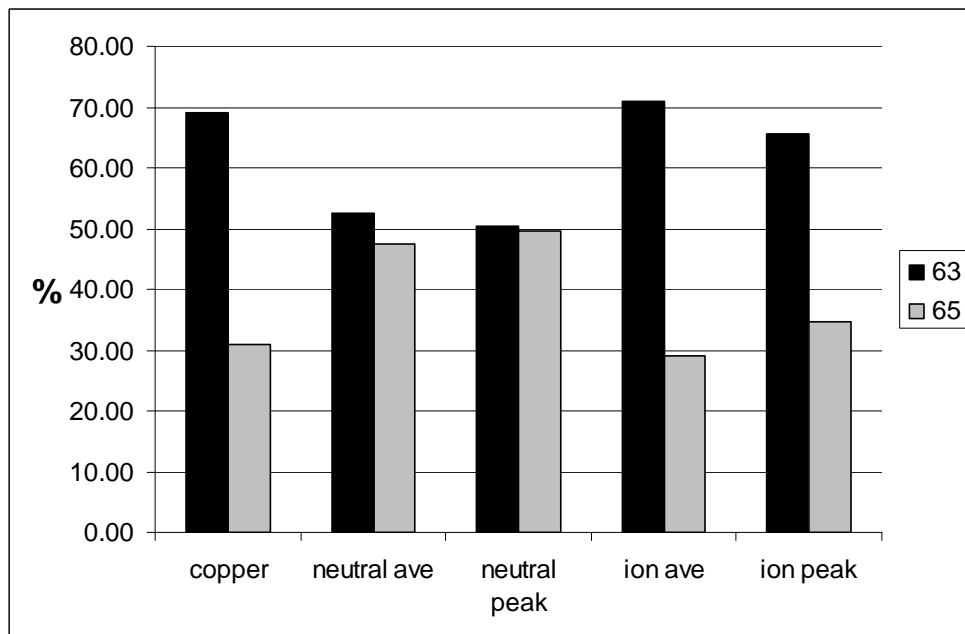

Figure 7. 63 amu and 65 amu- a comparison of the measured neutral and ion signals to the natural abundance of the two copper isotopes. Average signals (neutral ave, ion ave) and peak signals (neutral peak, ion peak) are shown.

Figure 7 compares the natural abundance of the two isotopes of copper [21] to the relative percentage of mass 63 amu and mass 65 amu observed when analysing either the neutral or ionic species produced by laser ablation of copper. Two different methods were employed to determine the relative abundance of 63 amu and 65 amu species within the vacuum chamber; measuring the average partial pressure signal of each mass during laser firing, or maximum peak signal for each mass during laser firing. These two methods were applied to the analysis of neutral and ionic species. It can be seen that the average ion signal provides the closest correlation to the natural abundance of the two copper isotopes. A proposed reason for this mismatch in the neutral signals may be that pump oil fragments provide extra contributions to the partial pressures recorded for 63 and 65 amu. As the quadrupole has integer mass resolution it is extremely difficult to ascertain the true nature of the particles contributing to the partial pressure scans of 63 and 65 amu with the current experimental configuration.

3.2 Fecralloy

Fecralloy is an alloy of iron (72.8%), chromium (22%), aluminium (5%), and trace amounts of zirconium and yttrium (≈0.1%). Simultaneous LIBS/LAMS analysis of Fecralloy was conducted to determine whether either technique would detect small trace amounts of minor elements within a major element matrix. The m/z peaks monitored using LAMS were: Fe - 56 amu; Cr - 52 amu; Al – 27 amu; Z - 89 amu and Y - 90 amu. Figures 8 and 9 show the partial pressures versus scan number for Fecralloy ions and neutrals respectively. It can be seen that the iron, aluminium and chromium peaks are well resolved whilst the minor elements, zirconium and yttrium, are just discernable above the background noise.

Figure 10 shows the LIBS spectrum of Fecralloy captured in the 301 - 313.5 nm range using the 2400 gmm^{-1} diffraction grating. This wavelength range was chosen as all the components of Fecralloy have strong emission lines within this region. The iron, aluminium and chromium are clearly seen, whilst the zirconium and yttrium cannot be resolved above the background noise. Due to matrix effects and self absorption within the plasma plume, the accurate composition of Fecralloy cannot be determined from the LIBS spectrum without the use of a set of calibration standards.
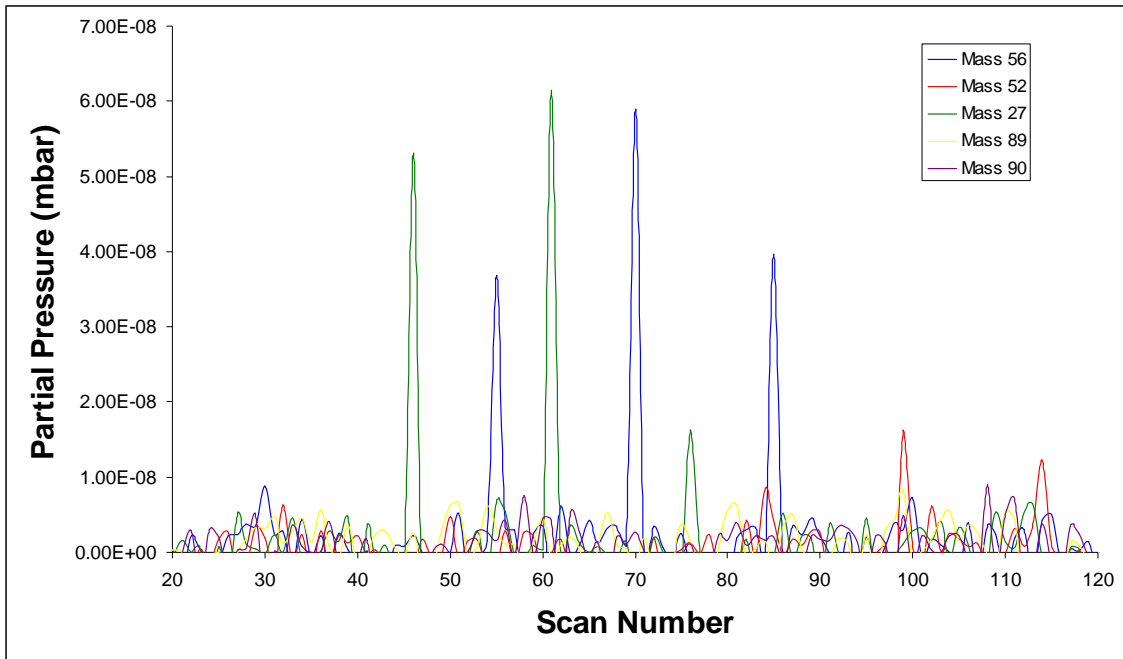
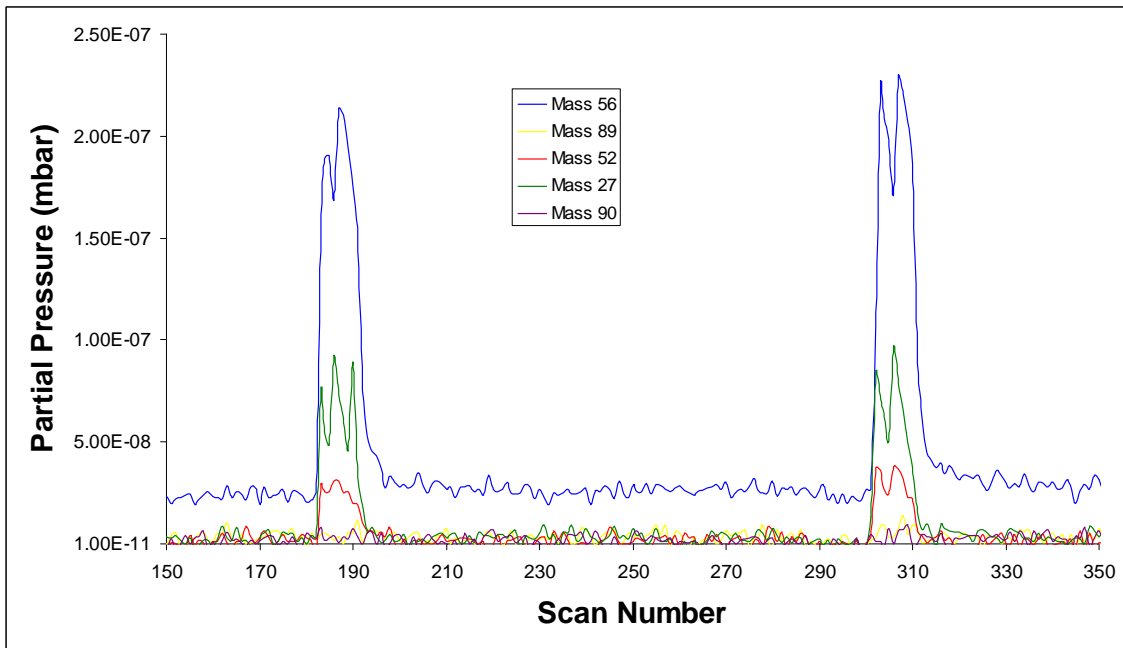Figure 8. Partial pressure versus scan number - Fecralloy ions.

Figure 9. Partial pressure versus scan number - Fecralloy neutrals.
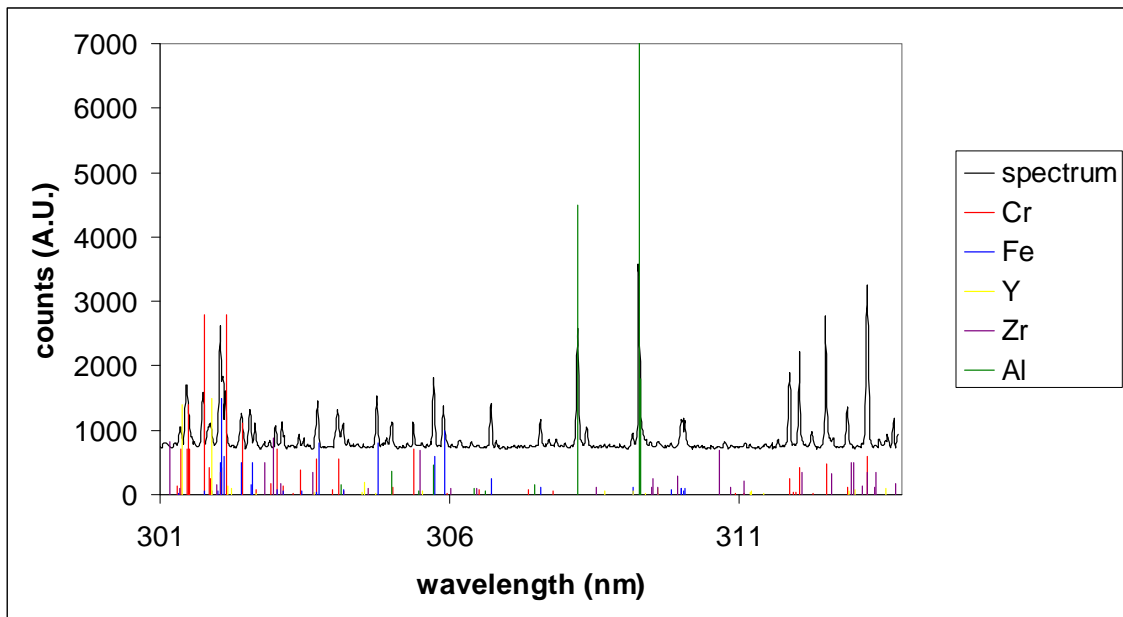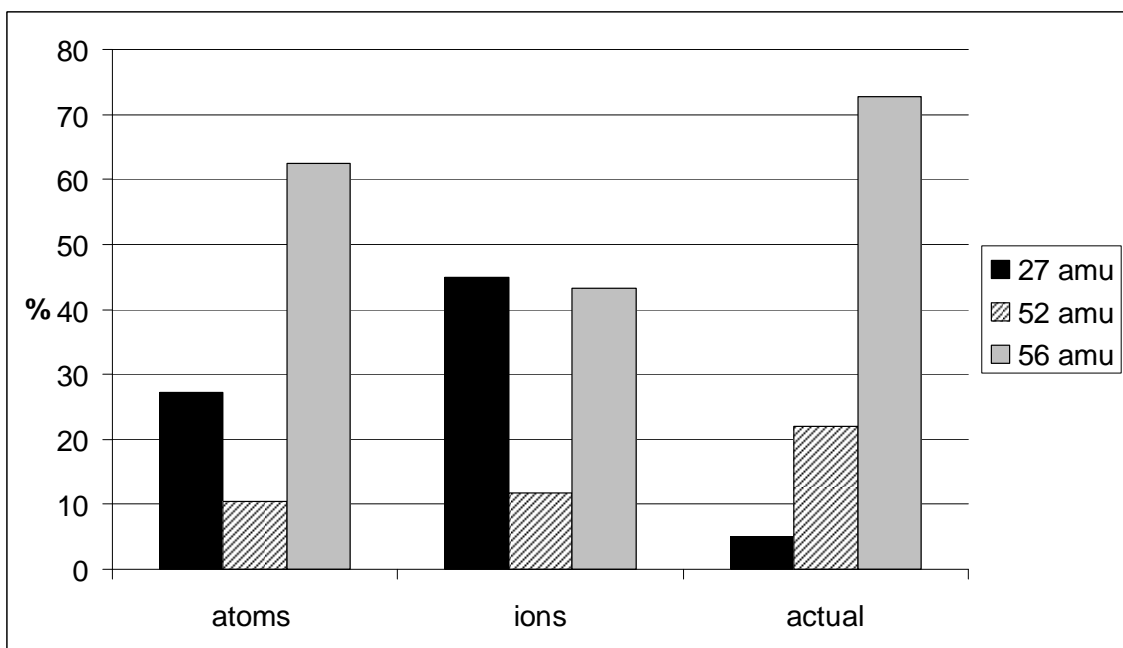
14

Figure 10. LIBS spectrum of Fecralloy.

Fig 11. Percentage composition of major elements of Fecralloy as determined from neutrals (left), and ions (middle) compared to manufacturer's given composition (right).

Figure 11 shows the percentage composition of Fecralloy as determined by monitoring the neutral and ionic ablation species, compared to the manufacturers' stated composition. If the ratio of iron to chromium is considered, then it can be seen that the ion signal ratio is close to that of the manufacturers' specification (approximately

3.5:1), whereas the neutral signal ratio (approx 6:1) is greater by almost a factor of 2. The aluminium percentages as determined from both neutral and ion species analysis show a large discrepancy when compared with the actual stated composition. The perceived elevated percentage of aluminium may be due to the fact that the natural oxide of Fecralloy is Al_2O_3 (alumina) [22], and this surface layer will contribute to the disproportionate amount of aluminium recorded.

4. Conclusion

Although not situated in an optimum sampling position, the RGA is able to detect small concentrations of material that the LIBS system has difficulty detecting. By investigating laser ablation of copper and Fecralloy it has been shown that the direct analysis of the ions produced by the ablation process yields a more accurate compositional determination than analysis of the neutral species.

The RGA was found to be too sensitive to chamber contamination when applied to analysis of neutral species. Pump oil molecules present within the chamber are ionised by the RGA ion source along with the ablated analyte neutrals. These high molecular weight long chain hydrocarbons have complex cracking patterns that can contribute a significant increase in the partial pressure signals recorded for a large range of masses. In the case of the 2 peaks that were monitored during the copper study (63 and 65 amu), it is now believed that the inclusion of $C_5H_3^+$ and $C_5H_5^+$ pump oil fragments has led to erroneous results when using the RGA with its associated hot filament ion source. Even though a fore-line oil filter was incorporated in the system it is known that oil molecules can still backstream into the vacuum chamber. These molecules tend to adsorb on to all the internal chamber surfaces; at a pressure of 10^{-6} mbar, there are approximately 10^6 molecules adsorbed on the walls of the system for each molecule in the gas phase [23]. During the ablation process, the expanding plume promotes electron/ion-stimulated desorption of oil contamination from interior chamber surfaces, and it is these molecules that are subsequently ionised and then analysed by the RGA. The limitations imposed by the relatively slow scan speed of the quadrupole mass spectrometer could be overcome by using an expensive Time of Flight mass spectrometer. The synchronisation of the RGA mass scan to the transient laser pulse has to be addressed if quadrupole LAMS is to be a used as an accurate, reproducible analytical technique.

LIBS was found to be unable to detect trace amount of zirconium and yttrium in Fecralloy, but proved to be unaffected by the pump oil vapour contamination in the process chamber, providing unambiguous elemental analysis of the major components of Fecralloy.

References:

[1]   J.M. Vadillo, J.J. Laserna, Laser-induce plasma spectrometry: truly a surface analytical tool, Spectrochimica Acta Part B 59 (2004) 147-161.

[2]   D.A. Rwak, B.C. Castle, B.W. Smith, J.D. Winefordner, Recent Trends and the Future of Laser-Induced Plasma Spectroscopy, Trends in Analytical Chemistry 17 (1998) 453-461.

[3]   J. Vrenegor, R. Noll, V. Sturm, Investigation of matrix effects in laser-induced breakdown spectroscopy plasmas of high-alloy steel for matrix and minor elements, Spectrochimica Acta Part B 60 (2005) 1083-1091.

[4]   A.M. El Sherbini, TH. M. El Sherbini, H. Hegazy, G. Cristoferetti, S. Legnaioli, V. Palleschi, L. Pardini, A. Salvetti, E. Tognoni, Evaluation of self-absorption coefficients of aluminium emission lines in laser-induced breakdown spectroscopy measurements, Spectrochimica Acta Part B 60 (2005) 1573-1579.

[5]   V. Lazic, R. Barbini, F. Calao, R. Fantoni, A. Palucci, Self-absorption model in quantitative laser induced breakdown spectroscopy measurements on soils and sediments, Spectrochimica Acta Part B 56 (2001) 807-820.

[6]   D. Bulajic, M. Corsi, G. Cristoferetti, S. Legnaioli, V. Palleschi, A. Salvetti, E. Tognoni, A procedure for correcting self absorption in calibration free-laser induced breakdown spectroscopy, Spectrochimica Acta Part B 57 (2002) 339-353.

[7]   B. Sallé, D.A. Cremers, S. Maurice, R.C. Wiens, Laser-induced breakdown spectroscopy for space exploration applications: Influence of the ambient pressure on the calibration curves prepared from soil and clay samples, Spectrochimica Acta Part B 60 (2005) 479-490.

[8]   P. Stavropoulos, C. Palagas, G.N. Angelopoulos, D.N. Papamantellos, S. Couris, Calibration Measurements in laser-induced breakdown spectroscopy using nanosecond and picosecond lasers, Spectrochimica Acta Part B 59 (2004) 1885-1892.

[9]   P. Yaroshchyk, D. Body, R.J.S. Morrison, B.L. Chadwick, A semi-quantitative standard-less analysis method for laser-induced breakdown spectroscopy, Spectrochimica Acta Part B 61 (2006) 200-209.

[10]   J. S. Becker, Applications of inductively coupled plasma mass spectrometry and laser ablation inductively coupled plasma mass spectrometry in materials science, Spectrochimica Acta Part B 57 (2002) 1805-1820.

[11]   C. J. Scadding, R. J. Watling, A. G. Thomas, The potential of using laser ablation inductively coupled plasma time of flight mass spectrometry (LA-ICP-TOF-MS) in the forensic analysis of micro debris, Talanta 67 (2005) 414-424.

[12]   M. Bi, A.M. Ruiz, I. Gornushkin, B.W. Smith and J. D. Winefordner, Profiling of patterned metal layers by laser ablation inductively coupled plasma mass spectrometry (LA-ICP-MS) , Applied Surface Science 158 (2000) 197-204.

[13]   R. Bugoi, B. Constantinescu, C. Neelmeijer, F. Constantin, The potential of external IBA and LA-ICP-MS for obsidian elemental characterization, Nuclear Instruments and Methods in Physics Research Section B 226 (2004) 136-146.

[14]   J. J. Corr, P. Kovarik, B. B. Schneider, J. Hendrikse, A. Loboda, T. R. Covey, Design Considerations for High Speed Quantitative Mass Spectrometry with MALDI Ionization , Journal of the American Society for Mass Spectrometry 17 (2006) 1129-1141.

[15]   Z. Liu, K. L. Schey, Optimization of a MALDI TOF-TOF mass spectrometer for intact protein analysis, Journal of the American Society for Mass Spectrometry 16 (2005) 482-490.

[16]   L. Matus, M. Seufert, K. P. Jochum, Ion yield of a laser plasma mass

spectrometer, International Journal of Mass Spectrometry and Ion Processes 84 (1988) 101-111.

[17]   S. Lazare, W. Guan, D. Drillhole, High sensitivity quadrupole mass spectrometry of neutrals sputtered by UV laser ablation of polymers, Applied Surface Science 96-98 (1996) 605-610.

[18]   M.C. Kelly, G.G. Gomlak, V.G. Panayotov, C. Cresson, J. Rodney, B.D. Koplitz, Energetics of pulsed laser ablation species as determined by quadrupole and time-of-flight mass spectrometry, Applied Surface Science 127-129 (1998) 988-993.

[19]   C.C Garcia, J.M Vadillo, S. Palanco, J. Ruiz, J.J. Laserna, Comparative analysis of layered materials using laser induced plasma spectroscopy and laser-ionisation time-of-flight mass spectrometry, Spectrochimica Acta Part B 56 (2001) 923-931.

[20]   M. Kuzuya, Y. Ohoka, H. Katoh, H. Sakanashi, Application of a quadrupole mass filter to laser ionisation mass spectrometry: synchronisation between the laser pulse and the mass scan, Spectrochimica Acta Part B 53 (1998) 123-129.

[21]   E. de Hoffmann, V. Stroobant, Mass Spectrometry Principles and Applications, second ed., John Wiley and Sons 2003. Table of Isotopic Abundances, 374-379.

[22]   D. Naumenko, W. J. Quadakkers, A. Galerie, Y. Wouters and S. Jourdain, Parameters affecting transient oxide formation on FeCrAl based foil and fibre materials, Materials At High Temperatures 20 (2003) 287–293.

[23]   J.L. de Segovia, A review of electron stimulated desorption processes influencing the measurement of pressure or gas composition in ultra high vacuum systems, Vacuum, 47 (1996) 333-340.